Bistable gaits and wobbling induced by pedestrian-bridge interactions

Igor V. Belykh, Russell Jeter, and Vladimir N. Belykh

Citation: Chaos **26**, 116314 (2016); doi: 10.1063/1.4967725
View online: http://dx.doi.org/10.1063/1.4967725
View Table of Contents: http://scitation.aip.org/content/aip/journal/chaos/26/11?ver=pdfcov
Published by the AIP Publishing

Bistable gaits and wobbling induced by pedestrian-bridge interactions

Igor V. Belykh,[1] Russell Jeter,[1] and Vladimir N. Belykh[2,3]
[1]*Department of Mathematics and Statistics and Neuroscience Institute, Georgia State University, 30 Pryor Street, Atlanta, Georgia 30303, USA*
[2]*Department of Control Theory, Lobachevsky State University of Nizhny Novgorod, 23, Gagarin Ave., Nizhny Novgorod 603950, Russia*
[3]*Department of Mathematics, Volga State University of Water Transport, 5A, Nesterov Str., Nizhny Novgorod 603950, Russia*

(Received 23 October 2016; accepted 31 October 2016; published online 30 November 2016)

Several modern footbridges around the world have experienced large lateral vibrations during crowd loading events. The onset of large-amplitude bridge wobbling has generally been attributed to crowd synchrony; although, its role in the initiation of wobbling has been challenged. To study the contribution of a single pedestrian into overall, possibly unsynchronized, crowd dynamics, we use a bio-mechanically inspired inverted pendulum model of human balance and analyze its bi-directional interaction with a lively bridge. We first derive analytical estimates on the frequency of pedestrian's lateral gait in the absence of bridge motion. Then, through theory and numerics, we demonstrate that pedestrian-bridge interactions can induce bistable lateral gaits such that switching between the gaits can initiate large-amplitude wobbling. We also analyze the role of stride frequency and the pedestrian's mass in hysteretic transitions between the two types of wobbling. Our results support a claim that the overall foot force of pedestrians walking out of phase can cause significant bridge vibrations. *Published by AIP Publishing.*
[http://dx.doi.org/10.1063/1.4967725]

The infamous opening-day oscillations of the London Millennium Bridge have significantly intensified interest in the dynamics of pedestrian locomotion and its interactions with lively bridges. Similar lateral wobbling of several other bridges in France, Japan, Portugal, Singapore, and Great Britain has also been documented. Although some aspects of the impact of crowd loading on the initiation of bridge wobbling have been clearly identified, the full picture of how an individual pedestrian contributes to collective lateral excitation of a bridge is far from being complete. In this paper, we seek to close this gap by analyzing the interaction of a single pedestrian with a ground structure such as a bridge. Our analysis indicates that this bi-directional interaction enables two distinct lateral gaits. Both gaits can correspond to pedestrians walking out of phase with the bridge, yet one gait produces significantly larger bridge oscillations than the other. We show that both gaits can stably co-exist such that a misstep can cause the pedestrian to switch gait, potentially causing wilder bridge oscillations. We also show that this bistability is controlled by the pedestrian mass, where heavier pedestrians are more prone to switching to the gait with stronger bridge wobbling. These results may shed light onto a strategy of crossing a lightweight, lively bridge with a heavy backpack. This is relevant to mountaineers traversing metallic ladders across giant crevasses on the Khumbu Icefall of Mount Everest, with a convenience-over-safety dilemma of having the backpack on or sending it over the ropes separately. In this regard, our study indicates that the extra weight may cause an abrupt onset of ladder lateral vibrations.

I. INTRODUCTION

The phenomenon known as the sympathy of pendulum clocks or Huygens' synchronization is the first historical example of collective behavior of mechanical oscillators.[1] In the Huygens' setup, two pendulum clocks, hanging from a wooden beam, showed an "odd" symmetry and ended up oscillating in perfect anti-phase.[2–4] As the clocks were oscillating in opposite directions, their forces compensated for each other, keeping the beam still. The pendulum clocks with the same coupling structure can also oscillate in-phase, inducing the anti-phase movement of the beam.[3–5] In recent years, collective behavior of mechanical oscillators has become an important topic with various engineering applications (see this Focus issue for more details[6]).

Modern bridges are an important example of interacting mechanical oscillators. In suspension bridges, suspension and load-bearing elements are coupled by the bridge girder such that all constituting parts can become oscillators in the presence of wind. The most famous example of an oscillating suspension bridge is the Tacoma Narrows Bridge[7–11] which collapsed in 1940 as a result of aerodynamics, even though the exact cause still remains unclear; at least, a definite description that meets unanimous experts' agreement has not been reached.[10,11] A more recent example of an oscillating girder bridge is the Volga Bridge in the Russian city of Volgograd which experienced long-wave resonance vibrations in 2011 and was closed for expensive repairs.[12] On foot bridges, pedestrians walking across a bridge interact with the bridge and may cause bridge oscillations when the frequency of the bridge falls into a critical frequency range of pedestrian walking. While wind and crowd loading of

bridges can have similar destabilizing effects,[13] the pedestrian-bridge interactions are bi-directional such that the pedestrians can adapt their behavior to the oscillations of the bridge.

The list of foot bridges, whose instability during a crowd loading event has been documented, includes the Toda Park Bridge,[14] Solférino Bridge,[15] the London Millennium Bridge,[16] the Maple Valley Great Suspension Bridge,[17] the Singapore Airport's Changi Mezzanine Bridge,[18] the Clifton Suspension Bridge,[19] and the Pedro e Inês Footbridge.[20]

The opening-day wobbling of the London Millennium Bridge in 2000 remains the most known example of pedestrian-induced oscillations which has attracted significant public interest.[21–23] A sudden onset of large-amplitude lateral wobbling of the London Millennium Bridge occurred when the number of pedestrians exceeded a critical value.[16] The abrupt onset of wobbling has been attributed to the phenomenon called synchronous lateral excitation or crowd synchrony,[16,24–28] although its role in the mechanism which is responsible for the initial sudden onset of bridge wobbling has been challenged.[29,30]

Recent papers[26–28] used coupled phase oscillators as simple models to explain how a synchronized crowd could initiate the wobbling of the London Millennium Bridge.[26–28] While phase oscillators account for the timing of pedestrian foot placement, they ignore an important component of pedestrian-bridge interaction: the impact of pedestrian foot forces.

In our recent paper,[31] we developed a bio-mechanically inspired model of pedestrians' response which captures the key properties of pedestrian lateral balance and the resulting foot forces on the bridge. This model is an extension of the inverted pendulum model of human balance[29,30] which had been successfully used to analyze the whole body balance of bipedal walking.[32–34] The use of the inverted pendulum models to describe pedestrian's gaits allowed us to predict the critical number of pedestrians required for the onset of wobbling of the London Millennium Bridge remarkably well.[31] Our results support the traditional observation that crowd synchrony was necessary for the London Millenium Bridge to experience large-amplitude wobbling.[31] Although, the exact cause of the initial onset of wobbling at least in the case of small amplitudes may be rooted into the ability of pedestrians to adapt their gait and maintain lateral balance while walking randomly.

In this paper, we study this adaptation mechanism by considering a single pedestrian walking on a lively bridge. We discover that pedestrian-bridge interactions can make the pedestrian walk with two distinct lateral gaits and be capable of switching between the gaits. Notably, both gaits can be out of phase with the bridge; however, one lateral gait is closer to moving in the opposite direction of bridge swaying, i.e., closer to anti-phase synchrony and, therefore, inducing larger amplitude wobbling. We give an analytical insight into the possible co-existence of two stable lateral gaits and analyze the role of gait frequency and the pedestrian's mass in hysteretic transitions between the two types of wobbling. Our results on the ability of a single pedestrian to initiate bridge wobbling when switching from one gait to another may give an additional insight into the initiation of wobbling without crowd synchrony as previously observed on the Singapore Airport's Changi Mezzanine Bridge[15] and the Clifton Suspension Bridge.[19] Both bridges wobbled during a crowd event; however, the averaged frequency of pedestrians' gaits was documented to be different from the bridge frequency, and the pedestrian walking showed no visible signs of synchrony.[29]

The layout of this paper is as follows. First, in Sec. II, we present and discuss the pedestrian-bridge model. In Sec. III, we study the dynamics of the pedestrian on a stationary ground, i.e., with no bridge movement. For a set of matching parameters, we derive exact equations for a unique stable limit cycle that corresponds to the pedestrian's lateral gait. In the general case of pedestrian system parameters, we give bounds on the existence of a stable limit cycle and its period. In Sec. IV, we study the full model with bridge movement and demonstrate that pedestrian-bridge interactions can induce bistable lateral gaits. We give analytical insight into the possibility of two bistable regimes of oscillations and support our analytical results with numerics. We also study hysteretic transitions between the gaits that can induce large-amplitude wobbling. Finally, Section V contains concluding remarks.

II. PEDESTRIAN-BRIDGE INTERACTION MODEL

We begin with the standard setup for modeling pedestrian-bridge interactions.[26,29–31] The model describes pedestrian-induced lateral vibrations of the bridge by a mass-spring-damper system (Fig. 1). The bridge of mass M can move in the horizontal direction with the damping coefficient d. The bridge motion is described by a damped linear oscillator, driven by side-to-side movement of a pedestrian. In our setup,[31] the pedestrian is represented by a self-sustained

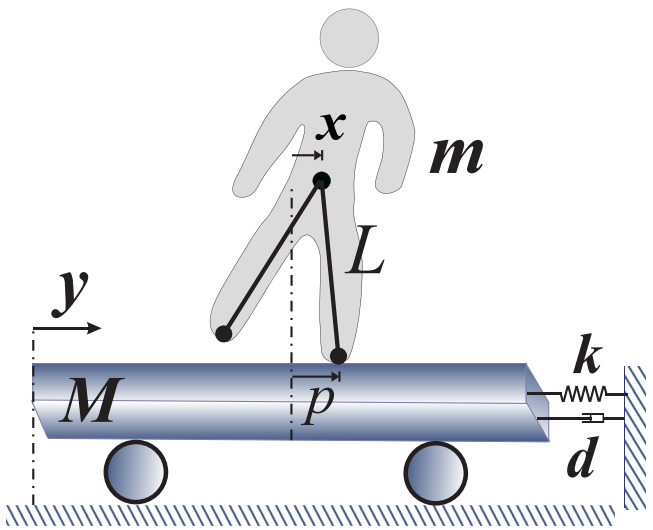

FIG. 1. Mechanical model of pedestrian-bridge interactions. The bridge is modeled by platform of mass M with one side attached to a rigid support via an elastic spring and a damper. Pedestrian lateral movement is modeled by an inverted pendulum of mass m with a massless leg of length L. x is the lateral position of pedestrian's center of mass. y accounts for lateral vibrations of the bridge. p is the lateral displacement of the center of pressure of the foot.

oscillator, where the pedestrian's gait and its adjustment to the bridge motion are modeled by an inverted pendulum model of human balance. The pedestrian-bridge model can be cast into the following form:

$$\ddot{x} + f(x,\dot{x}) = -\ddot{y}, \quad \ddot{y} + 2h\dot{y} + \Omega^2 y = -r\ddot{x}, \tag{1}$$

where x and y are horizontal movements of the center of mass of the pedestrian and the bridge, respectively. The feedback term $-\ddot{y}$ accounts for an inertia force on the pedestrian movement caused by the bridge movement. The pedestrian exerts sideways force $-r\ddot{x}$ on the bridge. The response of the pedestrian's gait to the bridge's oscillations and the gait adjustment are controlled by function $f(x,\dot{x})$. Parameters h and Ω are the damping and natural frequency of the bridge, respectively. Parameter $r = m/(M+m)$ represents the strength of pedestrian-bridge bi-directional interaction.

Function $f(x,\dot{x})$ which determines a self-sustained oscillatory mechanism of the pedestrian gait was introduced in Ref. 31 and has the form

$$f(x,\dot{x}) = \lambda[\dot{x}^2 + \nu^2\{a^2 - (x - p\cdot \hat{\text{sgn}}\, x)^2\}]\dot{x} - \omega^2(x - p\cdot \hat{\text{sgn}}\, x), \tag{2}$$

where $\hat{\text{sgn}}\, x = \{-1 \text{ if } x < 0;\ 1 \text{ if } x \geq 0\}$. The hat over the signum term indicates that in contrast to the standard signum function, which is 0 at $x = 0$, $\hat{\text{sgn}}\, x = 1$ at $x = 0$. However, when numerically studying the system (1)–(2), one may use the conventional signum function as x always differs from 0 due to finite numerical precision. The presence of the signum term in (2) accounts for reversing the direction of movement of the pedestrian center mass x when the pedestrian shifts the body's weight from one foot to the other. In (2), λ, ν, a, p, and ω are parameters, where λ corresponds to damping, ν and a control the self-excitatory mechanism of human walking, p is the horizontal displacement of the center of pressure of the foot, and $\omega = \sqrt{g/L}$ with g being the acceleration due to gravity and L being the distance from the center of mass to the center of pressure.

Notice that this system is obtained from an approximation $\sin x \approx x$ when $x/L \ll 1$. See Ref. 29 for the derivation of system (1)–(2) with $\lambda = 0$ from the mechanical setup of Fig. 1 and Newton's second law.

It is important to emphasize that the model (1)–(2) takes into account the role of the pedestrian footfall force and the adaptation of pedestrian's gait to bridge oscillations.

III. PEDESTRIAN MODEL: NO BRIDGE MOVEMENT

We begin by analyzing the pedestrian dynamics in system (1)–(2) in the absence of bridge movement, i.e., $\ddot{y} = 0$. Therefore, the equation of the pedestrian motion becomes

$$\ddot{x} + \lambda[\dot{x}^2 + \nu^2\{a^2 - (x - p\cdot \hat{\text{sgn}}\, x)^2\}]\dot{x} - \omega^2(x - p\cdot \hat{\text{sgn}}\, x) = 0. \tag{3}$$

In the following, we prove the existence of a stable limit cycle in system (3) and estimate its amplitude and period as a function of parameters ν, a, p, and ω. In particular, we will show that the period of pedestrian lateral gait, defined by the stable limit cycle, may vary from very small, when the pedestrian switches the body's weight from one foot to the other very quickly, to very large.

Readers who are willing to accept the results of this section without proof can proceed without loss of continuity to the description of pedestrian-bridge bistable interactions in Sec. IV.

A. Conservative case ($\lambda = 0$): A nonlinear center

In the absence of damping ($\lambda = 0$), system (3) turns into the conservative inverted pendulum model[30]

$$\ddot{x} - \omega^2(x - p\cdot \hat{\text{sgn}}\, x) = 0. \tag{4}$$

This piecewise linear system is widely used in modeling human balance from the biomechanics field.[30,32–34] It has a center fixed point at the origin and two saddles at $x = \pm p$ (see Fig. 2(a)). Each closed integral curve of the center fixed point is composed of two symmetric parts for $x > 0$ and $x < 0$ which are glued at the discontinuity line $x = 0$. As a result, the curves acquire a diamond-like shape. The family of integral curves lies inside a domain formed by the separatrices of the saddles. Each integral curve represents a periodic lateral movement of the pedestrian. While this simple conservative model proves to adequately describe the role of human balance,[30] it suffers from a drawback that the amplitude of the pedestrian's lateral gait is entirely controlled by the choice of the closed integral curve, associated with given initial conditions. Therefore, the pedestrian cannot adjust the lateral gait and walks at the gait which is dictated by the size of the first step, even though this step happened to be too big or too small. This issue becomes particularly important for the dynamics and analysis of the pedestrian-bridge system (1)–(2), and justifies the need of a structurally stable non-conservative model such as model (3). As the construction of (3) with $\lambda \neq 0$ is based on the knowledge of the conservative system (4), we perform a short analysis of system (4).

For convenience, system (4) can be cast into the form

$$\dot{x} = u, \quad \dot{u} = \omega^2(x - p\cdot \hat{\text{sgn}}\, x), \tag{5}$$

where the levels of integral curves (conservative quantities) are described by

$$u^2 - \omega^2(x - p\cdot \hat{\text{sgn}}\, x)^2 = C. \tag{6}$$

We are particularly interested in two values of C. $C = 0$ yields straight lines $u \equiv \dot{x} = \pm\omega(x - p\cdot \hat{\text{sgn}}\, x)$ that correspond to the separatrices of the two saddles at $x = \pm p$. The separatrices form a heteroclinic contour which corresponds to an infinite-period solution. In this case, the time for the pedestrian to switch weight from one leg to the other becomes infinite. $C = -\omega^2 a^2$ corresponds to the equation

$$u^2 - \omega^2(x - p\cdot \hat{\text{sgn}}\, x)^2 + \omega^2 a^2 = 0, \tag{7}$$

which yields a closed dashed curve (see Fig. 2(a)) which will be used later in the paper as the generating solution for a stable limit cycle in the non-conservative system (3) with

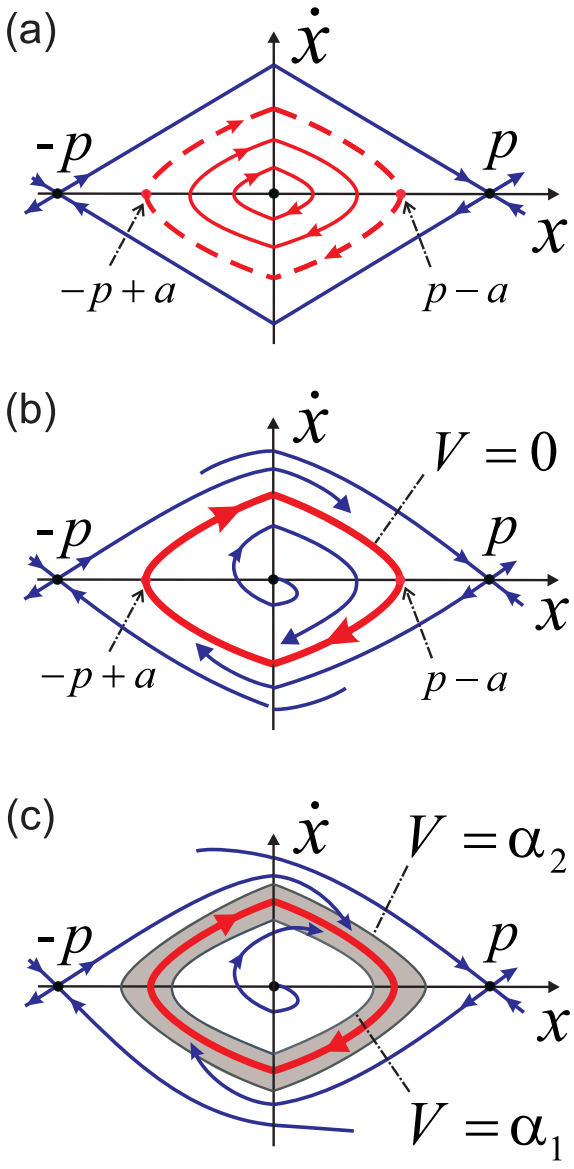

FIG. 2. Schematic phase portraits for the inverted pendulum model (3) without bridge movement. (a) Conservative system with $\lambda = 0$. Red lines indicate closed integral curves of the center fixed point at the origin. The dashed line corresponds to the generating solution for the limit cycle in the non-conservative system with $\nu = \omega$. (b) Non-conservative system with $\lambda \neq 0$ and $\nu = \omega$. The red closed curve corresponds to the stable limit cycle and the zero level of Lyapunov function V (cf. (8)). (c) The general case of non-conservative system with $\lambda \neq 0$ and $\nu \neq \omega$. Illustration of Theorem 2. The attracting annulus, depicted in gray, is bounded by two levels of the Lyapunov function, $V = \alpha_1$ and $V = \alpha_2$. The trajectories enter the annulus and approach the stable limit cycle.

$\lambda \neq 0$. The maximum amplitude of the pedestrian lateral gait corresponding to this level function is $x = p - a$; therefore, we assume that $0 < a < p$ throughout the paper. Negative values of a would push the trajectory outside of the absorbing domain (to the right from the saddle $x = p$) and make it increase without bound. From the pedestrian's perspective, this would correspond to the loss of balance and a fall. A more detailed analysis of the conservative model (4) and its fit to experimentally measured values of pedestrian lateral forces were reported in Refs. 29 and 30.

B. Non-conservative case: A stable limit cycle and its period

When damping is present such that $\lambda \neq 0$, system (3) can display a stable limit cycle whose equations can be derived in closed form in a specific case of $\nu = \omega$. The closed-form equation will allow us to calculate the period of the limit cycle, and therefore, the period of the pedestrian lateral gait. Below, we will perform this analysis, and then use the knowledge of the system dynamics for $\nu = \omega$ to estimate the amplitude and period of the limit cycle in the general case of $\nu \neq \omega$ where finding closed-form solutions is problematic.

1. Case $\nu=\omega$: Exact equations for the limit cycle

Substituting $\nu = \omega$ into system (3) yields

$$\dot{x} = u,$$
$$\dot{u} = -\lambda[\dot{x}^2 + \omega^2\{a^2 - (x - p\cdot \hat{\text{sgn}}\, x)^2\}]u + \omega^2(x - p\cdot \hat{\text{sgn}}\, x). \tag{8}$$

Theorem 1. [Explicit equations for the limit cycle].

1. System (8) has a unique stable limit cycle with coordinates $x(t)$ and $u(t)$ defined by

$$x = (p - a\cosh\omega t)\hat{\text{sgn}}\, x, \quad u = -a\sinh\omega t\cdot \hat{\text{sgn}}\, x. \tag{9}$$

2. This limit cycle has the period $T = 4\tau$, where

$$\tau = \frac{1}{\omega}\ln\left(p/a + \sqrt{(p/a)^2 - 1}\right). \tag{10}$$

The u- and x- amplitudes of the limit cycle are $\hat{A} = a\omega$ $\sinh(\omega\tau)$ and $\hat{B} = p - a$, respectively.

Proof. We use the closed curve (7) from the conservative case as a Lyapunov function candidate V to prove the uniqueness and stability of the limit cycle in system (8) in the region of interest $|x| < p$. Therefore, we set

$$V = u^2 - \omega^2(x - p\cdot \hat{\text{sgn}}\, x)^2 + \omega^2 a^2. \tag{11}$$

Note that $V = 0$ when x and u satisfy condition (7). Within the region of interest $|x| < p$, V is positive (negative) for x, u, lying outside (inside) the closed level curve (7).

The derivative of V along the trajectories of system (8)

$$\dot{V} = -2\lambda u^2 V \tag{12}$$

is negative (positive) definite when V is positive (negative). Therefore, the trajectories of system (8) converge to the level $V = 0$ (7) which represent a unique, stable limit cycle (see Fig. 2(b)).

The differential equation corresponding to $V = 0$:

$$(\dot{x})^2 = \omega^2(x - p\cdot \hat{\text{sgn}}\, x)^2 - \omega^2 a^2 \tag{13}$$

can be solved to obtain the explicit solution $x = \hat{\text{sgn}}\,(p - a\cosh\omega t)$. Consequently, differentiation yields $\dot{x} \equiv u = -a\sinh\omega t\cdot \hat{\text{sgn}}\, x$. This completes the proof of Part 1.

Given the explicit equations of limit cycle (9), the calculation of its period T is straightforward. For $t=0$, $x=p-a$ and $\dot{x}=0$. In one quarter τ of period T, the coordinates become

$$x=0,\quad \dot{x}=a\omega\sinh(\omega\tau). \tag{14}$$

Solving the initial value problem (14) yields (10). As τ corresponds to the time that the limit cycle spends in the fourth quadrant of the (x, u) plane, the period of the limit cycles is $T=4\tau$ (see Fig. 2(b)). Substituting (10) into the u-equation of (9) gives the value of $\hat{A}$. The maximum value of x is achieved at $t=0$ and defines amplitude $\hat{B}=p-a$. □

Remark 1.1. As (10) suggests, the period of the limit cycle T is controlled by parameters ω, p, and a, but is most sensitive to the ratio p/a. The period becomes zero (infinite) for $a=p$ $(a=0)$. Therefore, the non-conservative system (3) is capable of describing a full range of pedestrian lateral stride frequencies, from zero to infinite.

2. Case $\nu \neq \omega$: Estimates for the limit cycle period

For convenience, system (3) can also be rewritten in the form

$$\begin{aligned}\dot{x}&=u\\ \dot{u}&=-\lambda[\dot{x}^2+\nu^2\{a^2-(x-p\cdot \hat{\mathrm{sgn}}\, x)^2\}]u+\omega^2(x-p\cdot \hat{\mathrm{sgn}}\, x).\end{aligned} \tag{15}$$

In contrast to the previous case where $\nu=\omega$, we are unable to obtain the explicit equations for the limit cycle. However, we shall prove its existence and stability.

Theorem 2. [Bounds for the limit cycle].

System (15) has a stable limit cycle which lies in the annulus $R=\{\alpha_1<V<\alpha_2\}$, *where* V *is defined in (11) and* $\alpha_1=\min\{\omega^2(p^2-a^2),\nu^2(p^2-a^2)\}$ *and* $\alpha_2=\max\{\omega^2(p^2-a^2),\nu^2(p^2-a^2)\}$.

Proof. We use the Lyapunov function V, defined in (11), as a directing function for the system (15). Its derivative along the trajectories of system (15) is defined as follows:

$$\begin{aligned}\dot{V}/2&=u\dot{u}-\omega^2(x-p\cdot \hat{\mathrm{sgn}}\, x)\dot{x}\\ &=-\lambda(u^2+\nu^2[a^2-(x-p\cdot \hat{\mathrm{sgn}}\, x)^2])u^2.\end{aligned} \tag{16}$$

The derivative $\dot{V}$ is zero on the piecewise smooth ellipse $E:\{u^2+\nu^2[a^2-(x-p\cdot \hat{\mathrm{sgn}}\, x)^2]=0\}$ and is negative (positive) outside (inside) the ellipse E. To relate a sign of $\dot{V}$ to the levels of the directing function V, we need to determine two levels of V which inscribe and circumscribe the ellipse E. The level $V=\alpha_1$, where $\alpha_1=\min\{\omega^2(p^2-a^2),\ \nu^2(p^2-a^2)\}$, yields an ellipse that is inscribed within E. The level $V=\alpha_2$, where $\alpha_2=\max\{\omega^2(p^2-a^2),\nu^2(p^2-a^2)\}$, corresponds to an ellipse that is circumscribed about the ellipse E. Therefore, the derivative $\dot{V}$ on the level $V=\alpha_1$ $(V=\alpha_2)$ is either positive (negative) or becomes zero at the intersection points with the ellipse E. Hence, the annulus $R=\{\alpha_1<V<\alpha_2\}$, bounded by these two level curves, attracts the trajectories of (15) within the region of interest $|x|<p$, and contains a stable limit. □

Remark 2.1. For definiteness, assume that $\nu>\omega$. Then, the level of directing function $V=\alpha_1=\omega^2(p^2-a^2)$, and therefore, it corresponds to the limit cycle in the system (8), defined via the Lyapunov function (11). The period of this limit cycle is defined via (10). At the same time, the level $V=\alpha_2=\nu^2(p^2-a^2)$ corresponds to the limit cycle in the system (8) where ω is replaced with ν. Therefore, its period is determined by $T=\frac{4}{\nu}\ln\left(p/a+\sqrt{(p/a)^2-1}\right)$. As Theorem 2 proves, the limit cycle of system (15) with $\nu\neq\omega$ lies between the two levels; therefore, its period can be approximated by the period of the limit cycle in the system (8) with the mean value $(\omega+\nu)/2$:

$$T=\frac{8}{\omega+\nu}\ln\left(p/a+\sqrt{(p/a)^2-1}\right). \tag{17}$$

Figure 3 shows the limit cycle of system (15) with $\nu\neq\omega$ along with its acceleration time series.

IV. PEDESTRIAN-BRIDGE INTERACTIONS

Previous studies of the pedestrian-bridge system (1)–(2), where the pedestrian movement is described by the conservative inverted pendulum (2) with $\lambda=0$, derived approximate solutions for the pedestrian dynamics. This was done by assuming that the effect of a single pedestrian on the dynamics of a heavy bridge is fairly small; therefore, the bridge movement can be approximated by a simple harmonic solution with the natural bridge frequency Ω and a time lag from the beginning of the first step on the right foot to the start of the following bridge vibration cycle.[29] This assumption significantly simplifies the problem and reduces the analysis of the four-dimensional system (1)–(2) to the two

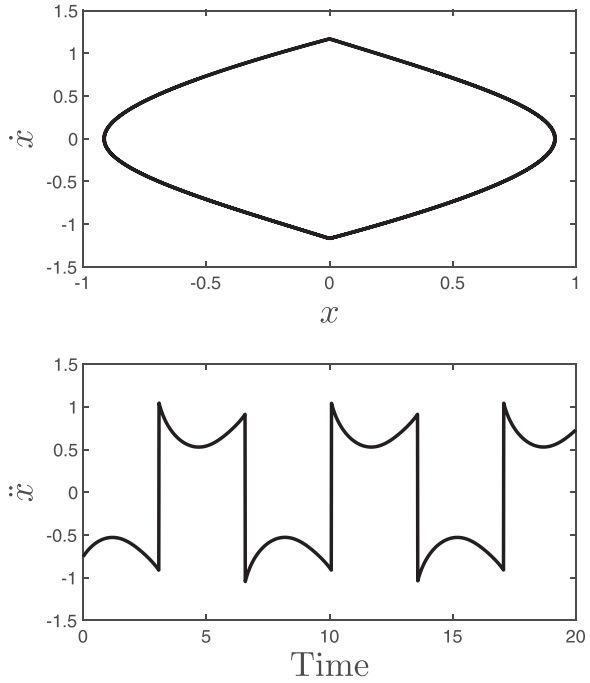

FIG. 3. Individual pedestrian model (3) with no bridge motion: numerics. The limit cycle and its acceleration time series. Parameters $\lambda=1$, $\omega=0.7$, $p=2$, $a=1$, and $\nu=0.66$.

dimensional equation for the pedestrian dynamics, driven by a sinusoidal external signal with frequency Ω. This practical, engineering approach yields approximations for pedestrian foot placement position consistent with the experimental data.[29] The use of a series solution with the fundamental frequency of the limit cycle in the isolated pedestrian system with no bridge motion as an external drive of the bridge equation may also give reasonable approximations within some range of parameters. However, these approaches, aimed at decoupling the dynamics of the pedestrian and the bridge, do not account for bi-directional interactions, and therefore cannot predict nonlinear effects due to the complex dynamics of the full four-dimensional system (1)–(2), including the bistability of pedestrian gaits.

A. Bistability of gaits: Analytical estimates

Our primary goal is to determine conditions on the parameters of the pedestrian-bridge system (1)–(2) that yield the co-existence of two limit cycles that correspond to distinct pedestrian lateral gaits. These two gaits are induced by pedestrian-bridge interactions and correspond to two regimes of wobbling with different amplitudes.

We follow the ideas proposed in our previous work on crowd dynamics[31] and seek solutions of system (1)–(2) that generate bistable wobbling. In our previous analytical study, we used Van-der-Pol-type models to describe pedestrians' gait and found harmonic periodic solutions that induce crowd synchrony and significant wobbling. However, the analysis of the interaction of the current piecewise-smooth pedestrian-bridge model (1)–(2) with "glued" solutions is much more challenging. As a result, we are unable to find closed-form solutions for both x and y, yet manage to give a qualitative argument for the possibility of bistable regimes. Obviously, such a complicated nonlinear system with switching right-hand sides (1)–(2) is not expected to be analytically tractable. However, our choice of the specific self-sustained oscillatory mechanism defined via $f(x,\dot{x})$ (2) allows us to conduct the assumed solutions through the "eye of the needle" of model (1)–(2) and obtain co-existence conditions.

Towards this goal, we will use an alternate form of pedestrian-bridge model (1)–(2)

$$\begin{aligned} &\ddot{x}+\lambda[\dot{x}^2+\nu^2\{a^2-(x-p\cdot \hat{\text{sgn}}\, x)^2\}]\dot{x}\\ &\quad -\omega^2(x-p\cdot \hat{\text{sgn}}\, x)=-\mu\ddot{y},\\ &\ddot{y}+2h\dot{y}+\Omega_0^2 y=-\mu\ddot{x}, \end{aligned} \tag{18}$$

obtained by setting $y=\mu y_{\text{new}}$ and $r=\mu^2$ in (1)–(2). By abuse of notation, we use the same symbol y for y_{new} in (18). A potential benefit of using the alternate form (18) is that setting μ to zero decouples both x- and y- equations and separates the dynamics of the pedestrian and the bridge.

As our analysis presented in Sec. III indicates, the limit cycle in the pedestrian model in the absence of bridge movement is composed of two symmetric parts which are defined by hyperbolic cosine and sine functions. Therefore, we also seek solutions of pedestrian-bridge model (18) in the form of the hyperbolic functions. The solution for the pedestrian movement $x(t)$ can be glued from one for $x(t)>0$ and its symmetric counterpart for $x(t)<0$ as the pedestrian switches body weight from one leg to the other when $x(t)$ crosses 0. $x(t)$ switching also affects the bridge movement $y(t)$ and makes its solution piecewise smooth. However, two discontinuity points at which two parts of the y-solution join together do not lie on the discontinuity line $x=0$.

Motivated by the form of solutions (9) in the pedestrian oscillator system (3) with no bridge movement, we use the following approximations of periodic solutions in the pedestrian-bridge system (18):

$$\begin{aligned} &x=(p-B\cosh\nu t)\hat{\text{sgn}}\, x, \quad \dot{x}=-B\nu\sinh\nu t\,\hat{\text{sgn}}\, x,\\ &y=\gamma-A\cosh(\nu t+\varphi)\cdot\hat{\text{sgn}}\, x, \quad \dot{y}=-A\nu\sinh(\nu t+\varphi)\cdot\hat{\text{sgn}}\, x, \end{aligned} \tag{19}$$

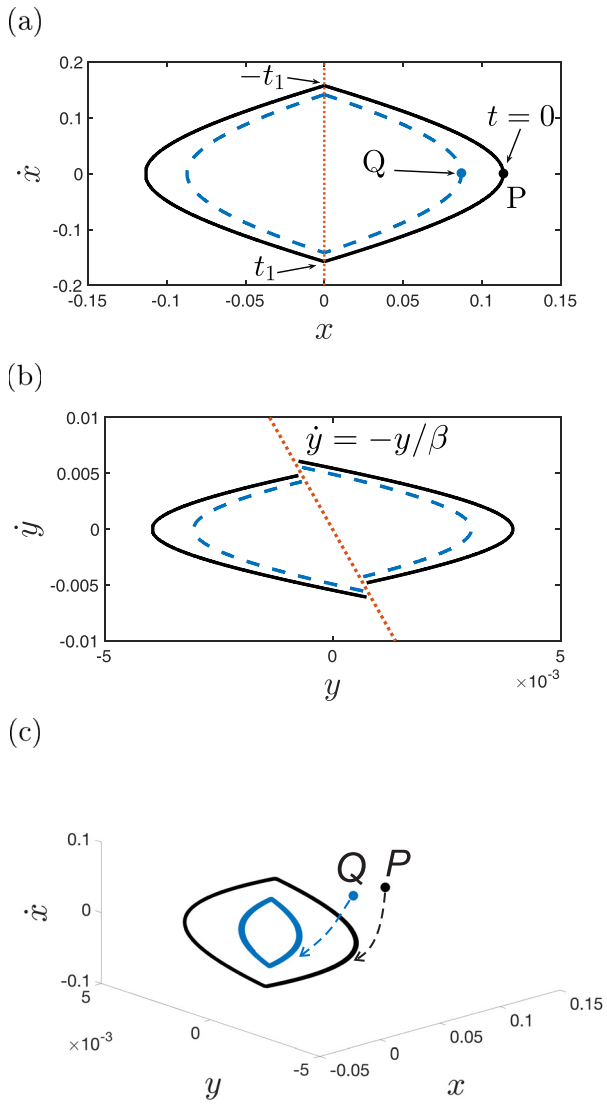

FIG. 4. Comparison of the analytical estimates [(a) and (b)] for the coexisting limit cycles to their numerically generated counterparts (c). (a)-(b) Theory: Solid (dashed) lines indicate the x- and y-solutions (40) with $A>0$, $B>0$, $\gamma>0$ ($A<0$, $B<0$, $\gamma<0$). Points P and Q correspond to one complete cycle of x-solutions. (c). Numerics: Continued from points P and Q, trajectories converge to two distinct limit cycles, depicted by black and blue (gray). The arrows schematically indicate the direction of convergence. Parameters $\lambda=0.1$, $\omega=0.7$, $p=0.3$, $a=0.2$, $\nu=0.67$, $\mu=0.11$, $h=0.1$, and $\Omega=1$.

where $-t_1 \le t \le t_1$ with time instant t_1 (t_2) corresponding to crossing the vertical line $x=0$ such that $\dot{x} > 0$ ($\dot{x} < 0$). With this choice of symmetric times $-t_1$ and t_1, the time $t=0$ corresponds to the crossing of the horizontal line $\dot{x}=0$ for $x>0$ (see Fig. 4(a)). A, B, γ, and φ are parameters whose values are to be determined. The discontinuity line $x=0$ in the $(x,\dot{x})$ plane corresponds to the discontinuity line

$$\dot{y} = -y/\beta \tag{20}$$

in the $(y,\dot{y})$ plane, where the parameter β is to be determined.

While the x-solution of system (19) is represented by a closed curve in the $(x,\dot{x})$ plane, the y-solution contains two discontinuous parts (see Fig. 4(b)) and cannot correspond to a limit cycle. As a result, the solutions (19) on the time interval $[-t_1, t_1]$ are parts of a transient solution that converges to a limit cycle as the system (18) has an absorbing domain and the origin is unstable. Even though it is transient, we will use solution (19) as a proxy for a limit cycle and show that there is a set of parameters of (18) that yields two co-existing solutions. We will use this argument as a qualitative justification for the appearance of bistable lateral gaits and bridge wobbling. We will also support this prediction by numerical simulations.

It is important to emphasize that the parameter ν, appearing in (19) as the argument of hyperbolic cosine function, is not the frequency of oscillations, as would be in the case of the cosine function. Similarly to the limit cycle in the non-conservative system (15) with no bridge movement, the frequency of oscillations, approximated by solutions (19), is essentially controlled by the parameters A and B and may range from zero to infinite (cf. Theorem 2).

We will take the following steps to show that there are two different sets of solutions (19), corresponding to the same set of parameters of system (18) and different pedestrian gaits. We will first relate the parameters β and φ, by calculating times t_1 and $-t_1$ and comparing the corresponding solutions $y(t_1)$ and $y(-t_1)$. We will then substitute the solutions (19) into the pedestrian-bridge system (18) to determine permissible values of parameters $A, B, \gamma, \varphi, \beta$ and their relation to the parameters of the pedestrian-bridge system. As a result, we will derive two balance equations for finding the unknown parameters $A, B, \gamma, \varphi, \beta$. As the solutions (19) contain hyperbolic functions, the balance equations also contain hyperbolic sine and cosine functions and can be resolved by applying the hyperbolic trigonometric identity. This will yield a relation between the squares of parameters A and B and, consequently, induce positive and negative permissible values of A, B, and γ. Thus, two combinations of the positive and negative values A, B, and γ will generate two different solutions (19).

We start by making the first step. It follows from (19) that the times t_1 and $-t_1$ taken by the solution to reach the discontinuity line $x=0$ can be calculated from $\cosh \nu t_1 = p/B$ such that

$$t_1 = \frac{1}{\nu} \cosh^{-1}(p/B). \tag{21}$$

Therefore, substituting the y-equation of (19) with $t=t_1$ and $t=-t_1$ into (20) gives the following two equations:

$$\begin{aligned} -\beta\nu A \sinh(\nu t_1 + \varphi) + \gamma - A\cosh(\nu t_1 + \varphi) = 0, \\ -\beta\nu A \sinh(-\nu t_1 + \varphi) + \gamma - A\cosh(-\nu t_1 + \varphi) = 0. \end{aligned} \tag{22}$$

It follows from (20) and (22) that

$$\beta = -\frac{1}{\nu}\tanh\varphi, \quad \gamma = A\cosh\nu t_1/\cosh\varphi = Ap/[B\cosh\varphi]. \tag{23}$$

We shall now demonstrate that equations (19) can indeed be solutions of the pedestrian-bridge system (18). Substituting (19) into the x- equation of (18) yields

$$\begin{aligned} &[\lambda\nu(a^2 - B^2)B + \mu A_s]\sinh\nu t \\ &\quad + \left[\left(1 - \frac{\omega^2}{\nu^2}\right)B + \mu A_c\right]\cosh\nu t = 0, \end{aligned} \tag{24}$$

where $A_c = A\cosh\varphi$ and $A_s = A\sinh\varphi$.

To make the analysis of the y-equation in (19) more manageable, we shift the variables $y \to y - \gamma$ in the pedestrian-bridge system (18) and then substitute solutions (19) into (18). Thus, we obtain the following equation

$$\begin{aligned} &[(\nu^2 + \Omega^2)A_s + 2h\nu A_c]\sinh\nu t \\ &\quad + [2h\nu A_s + (\nu^2 + \Omega^2)A_c + \mu\nu^2 B]\cosh\nu t = 0. \end{aligned} \tag{25}$$

To make equations (24) and (25) identities, we set the coefficients of the hyperbolic cosine and sine functions equal to 0. Therefore, it follows from (24) that

$$\begin{aligned} \lambda\nu(a^2 - B^2)B + \mu A_s = 0, \\ \left(1 - \frac{\omega^2}{\nu^2}\right)B + \mu A_c = 0, \end{aligned} \tag{26}$$

and equation (25) yields

$$\begin{aligned} (\nu^2 + \Omega^2)A_s + 2h\nu A_c = 0, \\ 2h\nu A_s + (\nu^2 + \Omega^2)A_c = -\mu\nu^2 B. \end{aligned} \tag{27}$$

Thus, the balance equations (26) and (27) can be viewed as "amplitude-phase" equations finding the unknown parameters A, B, γ, φ, and β. The quotes are used to indicate that none of the parameters $A, B, \gamma, \varphi, \beta$ alone determines the actual amplitude and phase of the x or y-oscillations (cf. system (19)).

Using the Kronecker method to solve the system (27) for A_s and A_c, we obtain

$$\begin{aligned} A_s = \frac{1}{\Delta}\begin{vmatrix} 0 & 2h\nu \\ -\mu\nu^2 B & \nu^2 + \Omega^2 \end{vmatrix} = 2\mu h\nu^3 B/\Delta, \\ A_c = \frac{1}{\Delta}\begin{vmatrix} \nu^2 + \Omega^2 & 0 \\ 2h\nu & -\mu B\nu^2 \end{vmatrix} = -\mu\nu^2(\nu^2 + \Omega^2)B/\Delta, \end{aligned} \tag{28}$$

where

$$\Delta = (\nu^2 - 2h\nu + \Omega^2)(\nu^2 + 2h\nu + \Omega^2). \tag{29}$$

Thus, we can calculate the unknown phase φ in the solution (19) from (28) as follows:

$$\begin{aligned} \tan\varphi &= \frac{A_s}{A_c} = -2h\nu/(\nu^2+\Omega^2), \\ \varphi &= -\tanh^{-1}\left[2h\nu/(\nu^2+\Omega^2)\right]. \end{aligned} \tag{30}$$

At the same time, solving system (26) for A_s and A_c gives

$$A_s = \lambda\nu(B^2 - a^2)B/\mu, \quad A_c = \left(\frac{\omega^2}{\nu^2} - 1\right)B/\mu. \tag{31}$$

Therefore, the phase φ can also be calculated from (31) as follows:

$$\tan\varphi = \frac{A_s}{A_c} = \lambda\nu(B^2 - a^2)\Big/\left(\frac{\omega^2}{\nu^2} - 1\right). \tag{32}$$

Equating the right-hand sides of equations (30) and (32), we obtain the value for the square of the amplitude coefficient B which is explicitly expressed via the parameters of the pedestrian-bridge system (18)

$$B^2 = a^2 - 2h\left(\frac{\omega^2}{\nu^2} - 1\right)\Big/[\lambda(\nu^2 + \Omega^2)]. \tag{33}$$

The hyperbolic trigonometric identity $\cosh^2\varphi - \sinh^2\varphi = 1$ yields $A^2 = A_c^2 - A_s^2$. Therefore, from (28), we obtain

$$A^2 = \mu^2\nu^4 B^2/\Delta. \tag{34}$$

For this condition to be true, the quantity Δ must be positive. Hence, we have the following constraint on the parameters of the pedestrian-bridge system (18)

$$\Delta = (\nu^2 - 2h\nu + \Omega^2)(\nu^2 + 2h\nu + \Omega^2) > 0. \tag{35}$$

Substituting (33) into (34) gives the explicit value for the square of the amplitude coefficient A

$$A^2 = \mu^2\nu^4\left[a^2 - 2h\left(\frac{\omega^2}{\nu^2} - 1\right)\Big/[\lambda\Delta(\nu^2 + \Omega^2)]\right]\Big/\Delta. \tag{36}$$

To fully determine the solutions (19) and the position of the discontinuity line $\dot{y} = -y/\beta$, we shall now calculate the remaining unknown constants γ, φ, and β.

We use (23) to calculate γ. Towards this goal, we need to calculate A/B from (34). This yields

$$A/B = \pm\mu\nu^2/\sqrt{\Delta}. \tag{37}$$

It follows from (28) that

$$A\cosh\varphi/B = -\mu\nu^2(\nu^2 + \Omega^2)/\Delta. \tag{38}$$

Comparing (37) and (38) gives

$$\cosh\varphi = \sqrt{\Delta}/(\nu^2 + \Omega^2).$$

Substituting this value and (37) into (23) yields the explicit formula for γ:

$$\gamma = \pm\mu\nu^2(\nu^2 + \Omega^2)p/\Delta. \tag{39}$$

Collecting the conditions on A, B, γ, φ, and β, we arrive at the following statement:

Theorem 3. [Co-existence of solutions].

1. The functions, approximating periodic oscillations in the pedestrian-bridge system (18),

$$\begin{aligned} x &= (p - B\cosh\nu t)\hat{\text{sgn}}\, x, \\ y &= \gamma - A\cosh(\nu t + \varphi)\cdot\hat{\text{sgn}}\, x, \end{aligned} \tag{40}$$

are solutions of the pedestrian-bridge system (18) on the interval $-t_1 \le t \le t_1$, where $t_1 = \frac{1}{\nu}\cosh^{-1}(p/B)$ if

$$\begin{aligned} A &= \pm\mu\nu^2\sqrt{\left[a^2 - 2h\left(\frac{\omega^2}{\nu^2} - 1\right)\Big/[\lambda\Delta(\nu^2+\Omega^2)]\right]\Big/\Delta}, \\ B &= \pm\sqrt{a^2 - 2h\left(\frac{\omega^2}{\nu^2} - 1\right)\Big/[\lambda(\nu^2+\Omega^2)]}, \\ \gamma &= \pm\mu\nu^2(\nu^2+\Omega^2)p/\Delta, \end{aligned} \tag{41}$$

$$\begin{aligned} \varphi &= -\tanh^{-1}[2h\nu/(\nu^2+\Omega^2)], \text{ and} \\ \Delta &= (\nu^2 - 2h\nu + \Omega^2)(\nu^2 + 2h\nu + \Omega^2) > 0. \end{aligned} \tag{42}$$

The discontinuity line at which the $y-$ solutions switch is defined by $\dot{y} = -y/\beta$, where $\beta = -\frac{1}{\nu}\tanh\varphi = 2h/(\nu^2+\Omega^2)$.

2. Two different combinations of parameters, $(A > 0, B > 0, \gamma > 0)$ and $(A < 0, B < 0, \gamma < 0)$ with the choice of the corresponding sign in the conditions (41), yield two sets of co-existing solutions $(x(t), y(t))$ that define two distinct lateral movements of the pedestrian (via $x(t)$) and two types of bridge wobbling (via $y(t)$).

Proof. The conditions (41) on A, B, and γ come from formulas (36), (33), and (39), respectively. The time t_1 that it takes the solution to reach the discontinuity line $x = 0$ is given in (21). The conditions (42) on φ and Δ are given in (30) and (29). The slope of the discontinuity line $\dot{y} = -y/\beta$ is defined via (23). □

Remark 3.1. While six possible combinations of positive and negative values of A, B, γ yield permissible solutions (40), only two combinations $(A > 0, B > 0, \gamma > 0)$ and $(A < 0, B < 0, \gamma < 0)$ generate solutions of practical interest. Other combinations either yield solutions that do not belong to the absorbing domain or coincide with the ones given by the two combinations.

Remark 3.2. The condition (42), $\Delta > 0$, gives a range of permissible values of parameters ν, h, and Ω that make $\gamma^2 > 0$ via (39) and therefore allow the co-existence of two solutions. It also follows from conditions (41) that permissible values of A and B exist if the discriminants are non-negative such that $a^2 > 2h\left(\frac{\omega^2}{\nu^2} - 1\right)/[\lambda(\nu^2 + \Omega^2)$.

Remark 3.3. The equations (40) do not explicitly use the equation for the discontinuity line $\dot{y} = -y/\beta$. However, the introduction of the discontinuity line and its formula explicit

in the parameters of the pedestrian-bridge system (18) is useful for illustrative purposes.

While the statement of Theorem 3 is completely rigorous, it only gives the conditions on the co-existence of transient solutions which can correspond to the co-existence of two limit cycles. Therefore, this result can be considered as a qualitative indicator for the possible co-existence of two stable limit cycles, corresponding to two bistable pedestrian lateral gaits and two different lateral oscillations of the bridge. To support this qualitative prediction, we plot two analytical solutions (40) with $(A>0, B>0, \gamma>0)$ and $(A<0, B<0, \gamma<0)$ in Figs. 4(a) and 4(b), and numerically continue these solutions from points P and Q. As Fig. 4(c) indicates, the trajectories starting from points P and Q on two analytical curves do converge to two different stable limit cycles, although the numerically computed limit cycles are smaller than the analytical estimates. These two limit cycles correspond to two co-existing pedestrian gaits which are both in anti-phase with bridge oscillations (Fig. 5).

B. Numerics: Basins of attraction and hysteretic transitions

In Fig. 4(c), we have used a set of parameters generating two co-existing gaits which are both in anti-phase with the bridge. In the following, we use a different set of parameters to demonstrate the co-existence of two pedestrian gaits such that one is close to in-phase with the bridge movement whereas the other is out-of-phase. Figure 6 shows two different projections of co-existing limit cycles. The limit cycle, depicted in black in Fig. 6, is characterized by the pedestrian balancing out-of-phase with the bridge oscillations. The limit cycle, depicted in blue (gray), corresponds to the pedestrian lateral movement closely following the bridge oscillations. Notice that the out-of-phase gait (black) induces large-amplitude wobbling whereas the in-phase gait only yields small amplitudes of bridge oscillations, even though the amplitude of the in-phase gait is larger (Fig. 7).

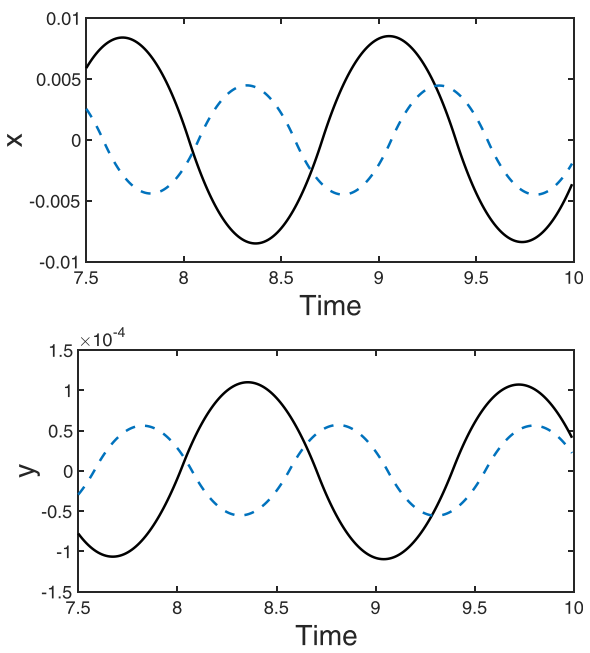

FIG. 5. Time-series corresponding to the limit cycles of Fig. 4(c). Solid black (dashed blue) lines indicate the time series generated by the large (small) limit cycle of Fig. 4(c). Note that both pedestrian gaits $x(t)$ are in anti-phase with the bridge movement $y(t)$, yet one gait produces larger bridge oscillations than the other.

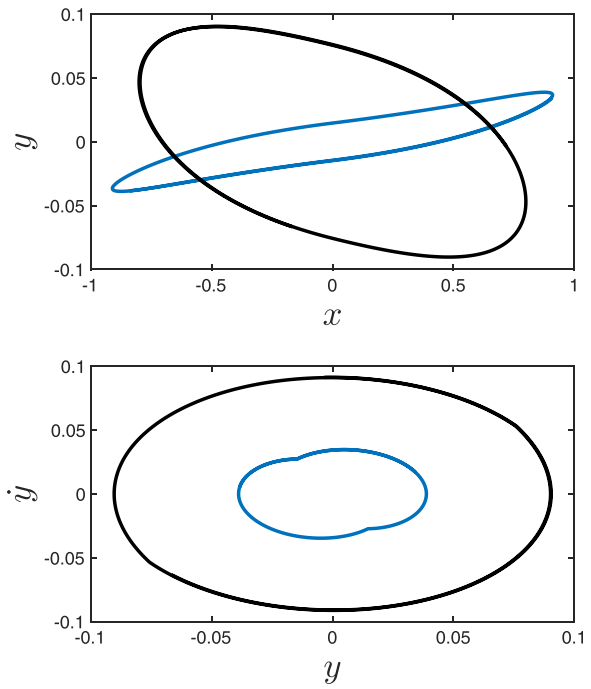

FIG. 6. Co-existence of two limit cycles, corresponding to two distinct gaits. The blue (gray) limit cycle corresponds to an in-phase gait with the bridge movement and induces low-amplitude wobbling. The black limit cycle corresponds to an out-of-phase movement which causes large-amplitude bridge oscillations. Parameters $\lambda=1$, $\omega=0.7$, $p=2$, $a=1$, $\nu=0.66$, $\mu=0.11$, $h=0.05$, and $\Omega=1$.

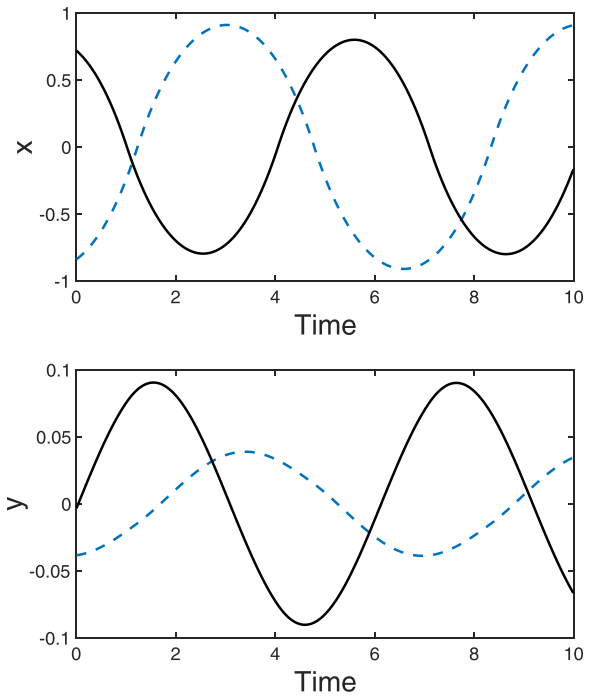

FIG. 7. Time-series corresponding to the limit cycles of Fig. 6. The pedestrian gait $x(t)$, which oscillates nearly in-phase with bridge wobbling $y(t)$ (dashed blue), co-exists with the out-of-phase gait and larger bridge oscillations (solid black).

The convergence to the two different limit cycles in Fig. 6 depends on both the system parameters and initial conditions. Figure 8 shows the long-term behavior of the system for various initial x and y values (with $\dot{x} = 0.01$ and $\dot{y} = 0$). The blue (dark) region corresponds to a set of initial conditions (x, y) for the onset of the in-phase gait and low-amplitude wobbling (cf. Fig. 6). The yellow (light) region indicates a set of initial conditions that yield the out-of-phase gait. The yellow region is significantly smaller, which suggests that the onset of the in-phase gait is more probable. However, the out-of-phase gait and the corresponding large-amplitude wobbling can appear from initial conditions close to the in-phase movement (note two narrow horizontal areas of the yellow basin of attraction whose tips are close to the diagonal line where both the pedestrian and the bridge start moving in phase). Hence, a small misstep may cause the in-phase gait to switch to the out-of-phase movement and induce potentially dangerous wobbling.

In addition to the dependence on initial conditions, the bridge-pedestrian system (18) can exhibit hysteretic behavior as one of the two stable limit cycles ceases to exist. Figure 9 illustrates this hysteretic transition as a function of parameter ν. According to the estimate (17) on the period of the pedestrian gait with no bridge motion, increasing ν increases the stride frequency of pedestrian walking. Therefore, we interpret ν as a control parameter for the gait frequency and study how the co-existence conditions change when ν varies. As Fig. 9 indicates, increasing ν from 0.6 leads to the emergence

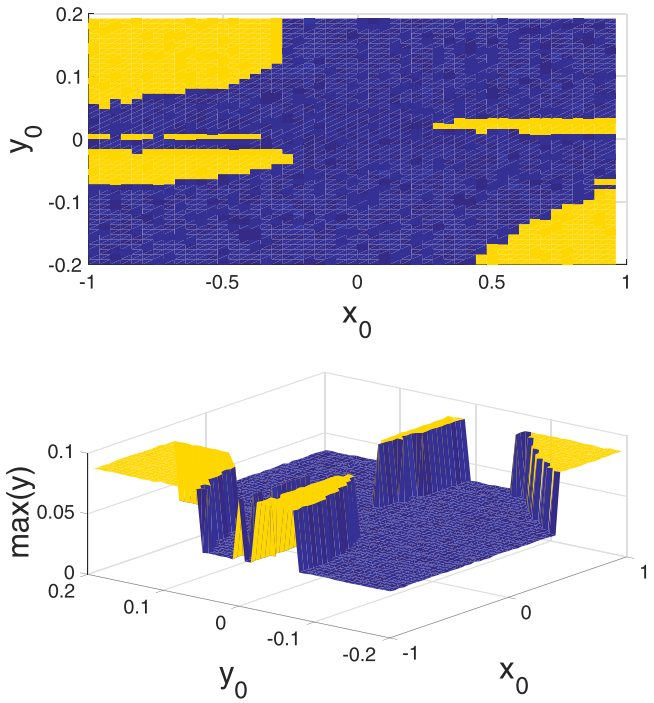

FIG. 8. Basin of attraction for two co-existing limit cycles. Yellow (light gray) corresponds to a set of initial conditions (x_0, y_0) for the convergence to the out-of-phase limit cycle (the black limit cycle of Fig. 6), and while blue (dark gray) indicates the convergence to the in-phase limit cycle (the blue limit cycle of Fig. 6). The 3-D diagram also displays the maximum amplitude of the established regime of wobbling. Notice the large amplitude wobbling, corresponding to the yellow basin of attraction of the out-of-phase cycle. Other initial conditions: $\dot{x} = 0.01$ and $\dot{y} = 0$. Parameters as in Fig. 6.

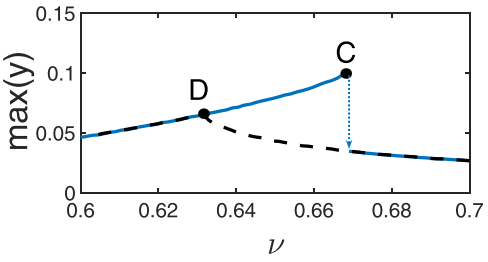

FIG. 9. Hysteretic transitions and bistability of wobbling as a function of ν. As ν increases (blue, solid curve), the system converges to the out-of-phase limit cycle, as the initial conditions are kept close to the limit cycle. At point C ($\nu \approx 0.67$), the out-of-phase limit cycle disappears, and the system switches to the in-phase limit cycle. For decreasing ν (black, dashed curve), the system remains in the basin of attraction for the in-phase limit cycle, until point D ($\nu \approx 0.63$) where the in-phase limit cycle disappears. Note that the dashed curve does not merge into point D, but ends abruptly, even though the gap is very small and visibly indistinguishable. Parameters as in Fig. 6, except for varying ν.

of small amplitude wobbling at point D and the disappearance of large-amplitude wobbling at point C such that the two types of wobbling co-exist in the region of ν between points D and C. Sweeping parameter ν from 0.6 to 0.7 and back yields the hysteretic curve of Fig. 9.

Figure 10 indicates that the bistability of two lateral gaits is also controlled by the pedestrian mass m such that increasing m leads to the emergence of the out-of-phase gait which co-exists with the in-phase gait. Therefore, heavier pedestrians are at higher risk of switching to the out-of-phase gait and, subsequently, initiating large-amplitude wobbling. These observations may offer guidance for choosing a best strategy for a hiker with a heavy backpack to traverse light rope hanging bridges in the Himalayas, where a heavier hiker might want to send the backpack over the ropes separately to reduce the risk of the abrupt onset of large bridge swaying. This might also be relevant to climbers crossing metallic ladders across giant crevasses when attempting to summit the Mount Everest.

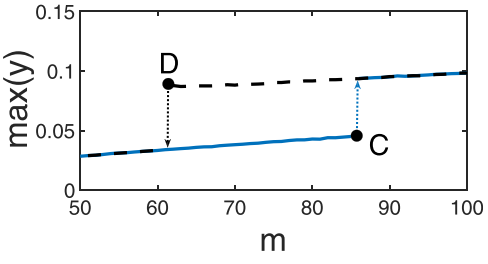

FIG. 10. Role of pedestrian mass m in the initiation of large-amplitude wobbling. Curves and notations are similar to Fig. 9. Notice that exceeding $m \approx 62$ induces the bistability of gaits, with a potential risk of large wobbling. Increasing pedestrian mass $m > 87$ inevitably induces large bridge oscillations. A hiker of mass $m = 70$ carrying a backpack with $m = 20$ may reduce the danger of large wobbling by traversing the bridge without the backpack on. This drops the overall mass from 90 to 70 and pushes the system into the bistable regime where the hiker might traverse the bridge with the in-phase gait. However, if the bridge already experiences large wobbling, decreasing the hiker load below $m = 87$ by removing a backpack will not necessarily cause the wobbling to dissipate due to the hysteretic effect. Parameters as in Fig. 6, except for varying $\mu = \sqrt{r}$, where $r = m/(M + m)$ with bridge mass $M = 5, 650$.

V. CONCLUSIONS

The list of modern pedestrian bridges, which showed instability due to crowd loading, is fairly long.[29] There are several views on what may trigger bridge wobbling, ranging from crowd synchrony[16,24–28] to a non-synchrony cause due to the asymmetry of the pedestrian-bridge behavior, with the lateral force increasing if the bridge moves away from the mass, but decreasing if the bridge moves towards it.[29,30]

In this paper, we have sought to address this question by studying the dynamics of pedestrian lateral locomotion and its interaction with a bridge. To isolate the effect of crowd loading, we have limited our attention to one single pedestrian on the bridge. We have used an inverted pendulum model of human balance to study changes in the pedestrian gait which are imposed by the bridge movement. However, this is a bi-directional interaction such that bridge oscillations are in turn controlled by the pedestrian movement. We first analyzed the dynamics theoretically and our analysis predicted that the pedestrian can stably exhibit two distinct lateral gaits, inducing two types of wobbling. We then verified this prediction numerically and revealed a variety of rich dynamics, induced by pedestrian-bridge interactions, including the co-existence of (i) in-phase and out-of-phase gaits; (ii) two out-of-phase gaits, and hysteretic transitions between them. We have shown that switching between the gaits can induce large-amplitude wobbling of the bridge. Our study suggests that potentially unsynchronized crowd dynamics, when each pedestrian can walk with two bistable lateral gaits, promise to lead to behavior that so far has not been adequately explained.

Our analytical study of the dynamics of the individual pedestrian with and without bridge motion contributes to the theory of non-smooth oscillators. Our theory may help engineers to (i) better understand the role of one pedestrian in initiation bridge wobbling, (ii) estimate a range of unsafe frequencies due to human responses to pedestrian bridge motion, and (iii) design robust bridges and other complex mechanical structures.

ACKNOWLEDGMENTS

We are thankful to John Macdonald and Alan Champneys both from the University of Bristol, UK, for the introduction to existing bio-inspired inverted pendulum models of pedestrian gait and useful discussions. This work was supported by the National Science Foundation (USA) under Grant No. DMS1616345 (to I.B. and R.J.) and by RSF under Grant No. 14-12-00811 and RFFI under Grant No. 15-01-08776 (to V.B.).

[1]C. Huygens, "Letter to de Sluse," in *Oeuveres Completes de Christian Huygens* (letters; no. 1333 of 24 February 1665, no. 1335 of 26 February 1665, no. 1345 of 6 March 1665) (Societe Hollandaise Des Sciences, Martinus Nijho, La Haye, 1665).
[2]M. Bennett, M. F. Schatz, H. Rockwood, and K. Wiesenfeld, Proc. R. Soc. London, A **458**, 563 (2002).
[3]A. Pikovsky, M. Rosenblum, and J. Kurths, *Synchronization, A Universal Concept in Nonlinear Sciences* (Cambridge University Press, Cambridge, 2001).
[4]J. P. Ramirez, L. A. Olvera, H. Nijmeijer, and J. Alvarez, Sci. Rep. **6**, 23580 (2016).
[5]E. V. Pankratova and V. N. Belykh, Eur. Phys. J. Spec. Top. **222**, 2509 (2013).
[6]I. V. Belykh and M. Porfiri, Chaos **26**, 116101 (2016).
[7]F. B. Farquharson *et al.*, Aerodynamic Stability of Suspension Bridges with Special Reference to the Tacoma Narrows Bridge, University of Washington Engineering Experimental Station, Seattle, Bulletin 116, Parts I to V, A series of reports issued since June 1949 to June 1954.
[8]K. Y. Billah and R. H. Scanlan, Am. J. Phys. **59**, 118 (1991).
[9]D. Green and W. G. Unruh, Am. J. Phys. **74**, 706 (2006).
[10]D. Cox, J. M. W. Curtiss, Jr., J. W. Edwards, K. C. Hall, D. A. Peters, R. H. Scanlan, E. Simiu, F. Sisto, and T. W. Stranac, in *A Modern Course in Aeroelasticity*, edited by E. H. Dowell (Springer, 2004).
[11]G. Arioli and F. Gazzola, Appl. Math. Model. **39**, 901 (2015).
[12]M. Brun, A. B. Movchan, I. S. Jones, and R. C. McPhedran, Phys. World **26**, 32 (2013).
[13]A. McRobie, G. Morgenthal, D. Abrams, and J. Prendergast, Phil. Trans. R. Soc. A **371**, 20120430 (2013).
[14]Y. Fujino, B. M. Pacheco, S. Nakamura, and P. Warnitchai, Earthquake Eng. Struct. Dyn. **22**, 741 (1993).
[15]F. Danbon and G. Grillaud, Footbridge 2005—Second International Conference, Venice, Italy (2005).
[16]P. Dallard, A. J. Fitzpatrick, A. Flint, S. Le Bourva, A. Low, R. M. Ridsdill-Smith, and M. Willford, Structural Eng. **79**, 17 (2001).
[17]S. Nakamura, Structural Eng. **88**, 22 (2003).
[18]J. M. W. Brownjohn, P. Fok, M. Roche, and P. Omenzetter, Structural Eng. **82**, 28 (2004).
[19]J. H. G. Macdonald, Proc. Inst. Civ. Eng. Bridge Eng. **161**, 69 (2008).
[20]E. Caetano, A. Cunha, C. Moutinho, and F. Magalhees, Eng. Struct. **32**, 1069 (2010).
[21]S. Zivanovic, A. Pavic, and P. Reynolds, J. Sound Vib. **279**, 1 (2005).
[22]V. Racic, A. Pavic, and J. M. W. Brownjohn, J. Sound Vib. **326**, 1 (2009).
[23]F. Venuti and L. Bruno, Phys. Life Rev. **6**, 176 (2009).
[24]S. Nakamura, J. Struct. Eng. ASCE **130**, 32 (2004).
[25]G. Piccardo and F. Tubino, J. Sound Vib. **311**, 353 (2008).
[26]S. H. Strogatz, D. M. Abrams, A. McRobie, B. Eckhardt, and E. Ott, Nature **438**, 43 (2005).
[27]S. Eckhardt, E. Ott, S. H. Strogatz, D. M. Abrams, and A. McRobie, Phys. Rev. E **75**, 021110 (2007).
[28]M. M. Abdulrehem and E. Ott, Chaos **19**, 013129 (2009).
[29]J. H. G. Macdonald, Proc. R. Soc. A **465**, 1055 (2009).
[30]M. Bocian, J. H. G. Macdonald, and J. F. Burn, J. Sound Vib. **331**, 3914 (2012).
[31]I. V. Belykh, R. Jeter, and V. N. Belykh, e-print arXiv:1610.05366.
[32]A. L. Hof, R. M. van Bockel, T. Schoppen, and K. Postema, Gait Posture **25**, 250 (2007).
[33]A. L. Hof, S. M. Vermerris, and W. A. Gjaltema, J. Exp. Biol. **213**, 2655 (2010).
[34]C. D. Mackinnon and D. A. Winter, J. Biomech. **26**, 633 (1993).